Inorg. Chem. **1992**, *31*, 770–774

Contribution from the Laboratoire de Chimie du Solide du CNRS, Université de Bordeaux I, 33405 Talence Cedex, France,
Fachbereich Chemie der Philipps-Universität und Wissenschaftliches Zentrum für Materialwissenschaften,
D-3550 Marburg, FRG, Institut Laue-Langevin, BP 156 X, 8042 Grenoble Cedex, France,
and Departamento de Quimica Inorganica, Universidad de la Laguna, 38200 Tenerife, Spain

A New Linear Chain Compound: Crystal and Magnetic Structures of $Tl_2MnF_5{\cdot}H_2O$

P. Nuñez,[†,‡] A. Tressaud,*[,‡] J. Darriet,[‡] P. Hagenmuller,[‡] G. Hahn,[§] G. Frenzen,[§] W. Massa,[§] D. Babel,[§]
A. Boireau,[‡,‖] and J. L. Soubeyroux[‖]

Received March 21, 1991

The crystal structure of a new liner chain compound $Tl_2MnF_5{\cdot}H_2O$ has been determined by X-ray diffraction. The structure has been refined down to $R = 0.034$ [*Cmcm* space group ($Z = 4$); unit cell constants $a = 9.688$ (2) Å, $b = 8.002$ (1) Å, and $c = 8.339$ (1) Å]. Manganese is located within elongated fluorine octahedra sharing two opposite corners to form infinite $(MnF_5)_n{}^{2n-}$ chains along the *c*-axis separated by Tl atoms and water molecules. In each chain, bridging Mn–F bonds are elongated: $Mn{-}F_{bridg} = 2.085$ Å, $Mn{-}F_{term} = 1.818/1.845$ Å, and the Mn–F–Mn angle is close to 180° as for the homologous Cs compound. Within a large temperature range the experimental magnetic properties can be fitted using the isotropic Heisenberg model for finite $S = 2$ spin chains in terms of intrachain antiparallel interaction. The best fitting is obtained for $J/k = -21.5$ K and $g = 1.99$. Below 28 ± 1 K 3D-antiferromagnetic ordering appears. The magnetic structure at 2 K has been refined down to $R = 0.09$ in the P*m′cm* space group; it corresponds to an antiparallel ordering in the *ab* plane between the Mn atoms located in neighboring chains.

Introduction

In spite of the large number of papers dealing with the structural properties of manganese(III) fluorides,[1] only a few recent publications are devoted to the magnetic ordering of these compounds.[2,3]

Mn(III) is a d^4 ion leading as a consequence of the high-spin configuration to a Jahn–Teller effect. Due to the existence of Tl_2AlF_5-type chain structures, which favor such a configuration, Mn(III)-based fluorides may be used as models for one dimensional magnetic systems.

Manganese(III) fluorides obtained from hydrofluoric solutions of trivalent manganese and of alkali-metal or alkaline-earth-metal salts are generally characterized by chains of axially elongated octahedra. The structures mainly consist of octahedra sharing trans-connected vertices, as in A_2MnF_5 (A = Li,[3] Na,[4] Rb,[5] Cs,[6] NH_4[7]), $A_2MnF_5{\cdot}H_2O$ (A = K,[8] Rb,[5,9] Cs[6,10]), $AMnF_5{\cdot}H_2O$ (A = Sr, Ba[11]) and $AMnF_4{\cdot}H_2O$ (A = K,[12] Rb,[13] Tl[14]). However, for larger cations various structures may be found, in which isolated octahedra are linked by hydrogen bonds forming a 3D-network: examples are given by tetrafluoromanganates(III) such as $AMnF_4{\cdot}2H_2O$ (A = Cs,[15] $(CH_3)_4N$,[13] NH_4[16]). A similar structure has been also described for $NaMnF_4{\cdot}xH_2O$ ($x = 2, 3$) with an unusual hydrogen-bridged geometry for the surrounding oxygen atoms.[17] On the other hand, it is possible to obtain from hot hydrofluoric solutions anhydrous $AMnF_4$ phases with $[MnF_6]$ octahedra sharing four equatorial corners, leading to layer structures (A = Tl,[18] Na[19]).

Pentafluoromanganates $A_2MnF_5{\cdot}xH_2O$ ($x = 0, 1$) have a pink color; their framework consists of chains of $[MnF_6]$ octahedra sharing trans corners. On the other hand tetrafluoromanganates(III) $AMnF_4{\cdot}xH_2O$ are dark brown. When they crystallize with one water molecule, the crystal structure is built up of chains of alternating trans-connected $[MnF_4F_{2/2}]$ and $[MnF_2F_{2/2}(H_2O)_2]$ octahedra.[1-4] When the number of water molecules exceeds one, chain structures are no longer observed, as the number of ligands is large enough to give rise to isolated octahedra $[MX_6]$ (X = F, H_2O) now linked by hydrogen bonds.

In previous papers,[2,18] we have reported the magnetic properties of several alkali-metal penta- and tetrafluoromanganates(III), in which the intrachain exchange constants J/k have been determined by fitting the susceptibility data to Fisher's equation[20] adapted by Smith and Friedberg[21] for finite chains with $S = 2$. A clear correlation between the calculated J/k values and both corresponding Mn–F–Mn angles and Mn–Mn distances has been deduced. As expected $|J/k|$ decreases for increasing departures of the Mn–F–Mn angles from 180° and increasing Mn–Mn distances.

Table I. Crystallographic Data for $Tl_2MnF_5{\cdot}H_2O$ (Mo Kα)

chem formula: $Tl_2MnF_5{\cdot}H_2O$	space group: Cmcm (N°63)
fw = 576.69	$T = 20 \pm 5$ °C
$a = 9.688$ (2) Å	$\rho_{obs} = 5.925$ g cm^{-3}
$b = 8.002$ (1) Å	$\rho_{calc} = 5.924$ g cm^{-3}
$c = 8.339$ (1) Å	$\mu = 251$ cm^{-1}, empirical cor
$V = 646.467$ Å^3	$R^a = 0.034$
$Z = 4$	$R_w = 0.022$

[a] $R = D/\sum F_o$; $D = |F_o - |F_c||$. $R_w = (\sum wD)^{1/2}/\sum wF_o^2$; $w \propto 1/\sigma_{F_o}^2$.

Table II. Atomic Coordinates of $Tl_2MnF_5{\cdot}H_2O$

atom	*x*	*y*	*z*
Tl	0.20826 (7)	0.29754 (10)	0.25
Mn	0.0	0.0	0.0
F1	0.0	–0.0006 (23)	0.25
F2	0.1876 (8)	0.0	0.0
F3	0.0	0.2305 (12)	0.0043 (14)
O	0.5	0.0507 (22)	0.25
H	0.5	0.1118	0.1666

In the present work we describe synthesis, structural determination, and magnetic characterization of the novel $Tl_2MnF_5{\cdot}H_2O$ phase.

Experimental Section

Synthesis. A solution of Mn(III) (0.01 mol) has been obtained by

---

[†] Universidad de la Laguna.

[‡] Universitê de Bordeaux I.

[§] Fachbereich Chemie der Philipps-Universität und Wissenschaftlichen Zentrum für Materialevissenschaften.

[‖] Institut Laue-Langevin.

(1) Massa, W.; Babel, D. *Chem. Rev.* **1988**, *88*, 275.
(2) Nuñez, P.; Darriet, J.; Bukovec, P.; Tressaud, A.; Hagenmuller, P. *Mater. Res. Bull.* **1987**, *22*, 661.
(3) (a) Pebler, J.; Massa, W.; Lass, H.; Ziegler, B. *J. Solid State Chem.* **1987**, *71*, 87. (b) Palacio, F.; Andres, M.; Esteban-Calderon, C.; Martinez-Ripoll, M.; Garcia-Blanco, S. *J. Solid State Chem.* **1988**, *76*, 33.
(4) Massa, W. *Acta Crystallogr.* **1986**, *C42*, 644.
(5) Günter, J. R.; Matthieu, J. P.; Oswald, H. R. *Helv. Chim. Acta* **1978**, *61*, 328.
(6) Hahn, F.; Massa, W. *Z. Naturforsch.* **1990**, *45b*, 1341.
(7) Sears, D. R.; Hoard, J. L. *J. Chem. Phys.* **1969**, *50*, 1066.
(8) Edwards, A. J. *J. Chem. Soc., A* **1971**, 2653.
(9) Bukovec, P.; Kaučič, V. *Acta Crystallogr.* **1978**, *B34*, 3339.
(10) Kaučič, V.; Bukovec, P. *Acta Crystallogr.* **1978**, *B34*, 3337.
(11) Massa, W.; Burk, V. *Z. Anorg. Allg. Chem.* **1984**, *516*, 119.
(12) Massa, W.; Baum, G.; Drueeke, S. *Acta Crystallogr.* **1988**, *C44*, 167.
(13) Kaučič, V.; Bukovec, P. *J. Chem. Soc., Dalton Trans.* **1979**, 1512.
(14) Nuñez, P.; Boireau, A.; Soubeyroux, J. L.; Tressaud, A.; Massa, W.; Babel, D. *Phys. Status Solidi A* **1991**, *127*, 505.
(15) Dubler, E.; Linowsky, L.; Matthieu, J. P.; Oswald, H. R. *Helv. Chim. Acta* **1978**, *60*, 1589.
(16) Andres, M. Thesis, University of Zaragoza (Spain), 1990.
(17) Massa, W.; Schmidt, R. E. *Z. Naturforsch.* **1990**, *45B*, 593.
(18) Nuñez, P.; Tressaud, A.; Grannec, J.; Hagenmuller, P.; Massa, W.; Babel, D.; Boireau, A.; Soubeyroux, J. L. *Z. Anorg. Allg. Chem.*, in press.
(19) Molinier, M.; Massa, W.; Khairoun, S.; Tressaud, A.; Soubeyroux, J. L. *Z. Naturforsch.*, in press.
(20) Fisher, M. E. *Am. J. Phys. Chem.* **1964**, *32*, 343.
(21) Smith, T.; Friedberg, S. A. *Phys. Rev.* **1968**, *176*, 660.

0020-1669/92/1331-0770$03.00/0

dissolving Mn_2O_3 in a hot 40% HF aqueous solution (15 mL). Mn_2O_3 was prepared as previously described.[22] Tl_2CO_3 (0.04 mol) was dissolved in a similar solution (15 mL). Both fresh solutions were cooled and then mixed together. The remaining solution was allowed to stand overnight at room temperature. A pink powder first appeared, which was filtered in order to improve the quality of the obtained crystals. The solution was kept at 5 °C for several days. Prismatic reddish-pink crystals were grown from this cold solution. Both powder and crystals were quickly washed successively in a 20% HF solution and in ethanol and then dried on a paper sheet in air. Powdered and crystalline samples exhibited identical X-ray diffraction (XRD) patterns.

X-ray Diffraction. Powder patterns of $Tl_2MnF_5 \cdot H_2O$ were recorded (Cu Kα radiation) at room temperature using Ge as internal standard. The lattice constants were in good agreement with those refined from 25 high-angle single-crystal reflections (Table I).

The crystal structure of $Tl_2MnF_5 \cdot H_2O$ was determined on a single crystal (0.09 × 0.09 × 0.17 mm^3) with a four-circle diffractometer CAD4 (Enraf-Nonius) using Mo Kα radiation and a graphite monochromator. The main crystallographic data are given in Table I. Starting from the structural model of $Rb_2MnF_5 \cdot H_2O$ as reference, the structure could be refined using anisotropic temperature factors for all atoms except hydrogen.

The positions of the H atoms have been selected from the neutron diffraction results (see below) and were kept at fixed positions chosen in order to yield an O–H distance of 0.85 Å, a realistic value for XRD. A fixed isotropic U = 0.06 Å was adopted for these H atoms. A careful empirical absorption correction was applied based on ψ scans on an optimized set of nine reflections. Then an extinction parameter $\epsilon = 4.4 \times 10^{-8}$ could be obtained by refining from the expression $F_c(\mathrm{corr}) = F_c(1 - \epsilon F_c^2/\sin\theta)$. Application of a weighting scheme $w = 1/\sigma^2(F_o)$ led to final R factors: R = 0.034 and R_w = 0.022 for 413 unique reflections. The resulting atomic parameters are given in Table II.

Low-temperature powder diffractograms were recorded down to 8 K on a Huber LT-Guinier diffractometer.

Magnetic Measurements. Magnetic measurements on $Tl_2MnF_5 \cdot H_2O$ were carried out from 1.8 to 300 K for both powder samples and single crystals using a SQUID magnetometer. Crystals were positioned parallel to the three crystallographic axes using Weissenberg photographs. The magnetic measurements were performed with an external magnetic field successively oriented along the three axes. Magnetic fields were applied up to 5 T.

Neutron Diffraction. Neutron diffraction patterns were carried out at the High Flux Reactor of the Institut Laue-Langevin (ILL) in Grenoble using a DIB powder diffractometer equipped with a large position-sensitive detector (PDS). Diffractograms were recorded with neutron wavelength λ = 2.522 Å in the range 4° < 2θ < 84°, between 1.5 and 300 K using a liquid-helium cryostat. The crystallographic structure was determined using the Rietveld profile refinement technique.[28-30]

Results and Discussion

Penta- and tetrafluoromanganates(III) can be prepared under quite close experimental conditions. Evidence can be given that the decisive parameter which governs the growth process is actually the reaction temperature. At low temperature (≈5 °C), the pink pentafluoromanganate is usually formed, whereas if the solution is kept at higher temperature (about 50 °C), the corresponding brown tetrafluoromanganate is obtained. Nevertheless, due to the unequivocal difference in color, it is possible to distinguish both phases from each other, even if they are simultaneously present.

In the Tl/Mn(III)/F/H_2O system we have isolated in fact three new phases which are different in composition and structure: $Tl_2MnF_5 \cdot H_2O$, $TlMnF_4 \cdot H_2O$, and $TlMnF_4$.

Table III. Selected Interatomic Distances (Å) and Angles (deg)[a]

Mn–F1	2.085 (1) (2×)	Mn–F3	1.845 (9) (2×)
Mn–F2	1.818 (7) (2×)	mean Mn-F	1.916
Tl–F1	3.124 (14)	Tl–F3^{v+vi}	3.541 (7) (2×)
Tl–F1^{i}	3.255 (9)	Tl–O	3.448 (10)
Tl–F2, F2^{ii}	3.171 (1) (2×)	Tl–O^{vii}	2.859 (13)
Tl–F2^{iii+iv}	2.826 (3) (2×)	mean Tl–F	3.131
Tl–F3, F3^{ii}	2.925 (8) (2×)		
F1–Mn–F2	90.0	F2–Mn–F3	90.0
F1–Mn–F3	89.0/91.0 (6)	Mn–F1–Mn	179.2 (3)
	Hydrogen Bonds		
O···F(3)$^{v+vi}$	2.750 (16)	F(3)··O··F(3)	100.9 (7)

[a] Symmetry operations: (i) $^1/_2 + x, {}^1/_2 + y, z$; (ii) $x, y, {}^1/_2 - z$; (iii) $^1/_2 - x, {}^1/_2 - y, -z$; (iv) $^1/_2 - x, {}^1/_2 - y, {}^1/_2 + z$; (v) $^1/_2 + x, {}^1/_2 - y, -z$; (vi) $^1/_2 + x, {}^1/_2 - y, {}^1/_2 + z$; (vii) $-^1/_2 + x, {}^1/_2 + y, z$.

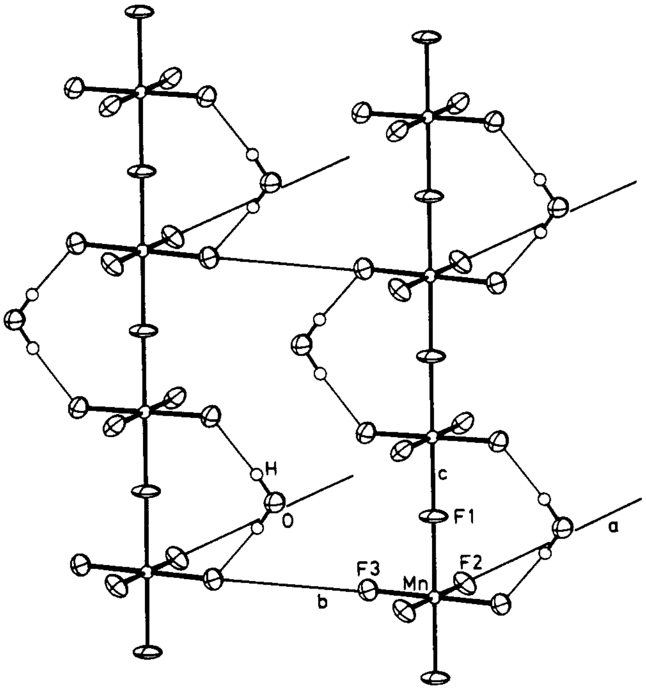

Figure 1. Structure of $Tl_2MnF_5 \cdot H_2O$. $(MnF_5)_n^{2n-}$ linear chains run along the c-axis. Water molecules are shown to link two nearest F3 atoms due to hydrogen bonds in a zigzag configuration (ORTEP drawing,[25] thermal ellipsoids at the 50% level).

Crystal Structure of $Tl_2MnF_5 \cdot H_2O$. $Tl_2MnF_5 \cdot H_2O$ crystallizes in the same orthorhombic *Cmcm* space group as $Rb_2MnF_5 \cdot H_2O$, which also has quite similar lattice parameters (a = 9.383 Å, b = 8.214 Å, c = 8.348 Å).[5,9] Both structures are isostructural with $Tl_2AlF_5 \cdot H_2O$.[31]

The structure of $Tl_2MnF_5 \cdot H_2O$ consists of infinite chains of trans-corner-connected octahedra $[MnF_4F_{2/2}]$ running parallel to the c-axis.

The $[MnF_6]$ octahedra (Figure 1, Table III) exhibit a strong elongation in the chain direction (Mn–F$_{ax}$ = 2.085 (1) Å, to compare with the mean Mn–F$_{eq}$ = 1.832 Å). This distortion can be largely attributed to the Jahn–Teller effect resulting from Mn^{3+} (high-spin d^4 configuration, ferrodistortive order), judging by comparison with the isostructural trans-chain Al compound $Tl_2AlF_5 \cdot H_2O$[31] with Al–F$_{ax}$ = 1.871 Å and Al–F$_{eq}$ = 1.775 Å). The bridging Mn–F–Mn angle within a chain is quasi-linear (179.2 (3)°). The crystal water molecules connect two neighboring octahedra belonging to the same chain: they alternate along the c-axis. It may be noted that the smaller bridging angle at F1 of 179.2° appears at the side opposite to the water molecule (Figure 1). The chains are packed in a tetragonal way (Fig. 2). The Tl atoms between the layers have CN = 12 (10 F and 2 O atoms) and form zigzag rows along the c-axis (Figure 2), the alternating displacements following those of the H_2O molecules.

---

(22) Moore, T. E.; Ellis, E.; Selwood, P. E. *J. Am. Chem. Soc.* **1950**, *72*, 856.
(23) Schmidt, R. E.; Birkhahn, M.; Massa, W. STRUX. Programm system zur Verarbeitung von Röntgendaten, Marburg, Ger, 1982.
(24) Sheldrick, G. M. SHELX76. Program for Crystal Structure Determination, Cambridge, England, 1976.
(25) Johnson, C. K. ORTEP: A Fortran Thermal Ellipsoid Plot Program for Crystal Structure Illustrations. Report ORNL-3794; Oak Ridge National Laboratory; Oak Ridge, TN, 1965.
(26) Cromer, D. T.; Mann, J. D. *Acta Crystallogr.* **1968**, *A24*, 321.
(27) Cromer, D. T.; Liberman, D. *J. Chem. Phys.* **1970**, *53*, 1891.
(28) Watson, R. E.; Varret, E. Program HOSFIT, unpublished work.
(29) Young, R. A.; Wiles, D. B. *J. Appl. Crystallogr.* **1981**, *14*, 149.
(30) Brown, P. J. *International Tables for Crystallography*, Vol. C, in press.
(31) Molinier, M.; Massa, W. Unpublished results, 1991.

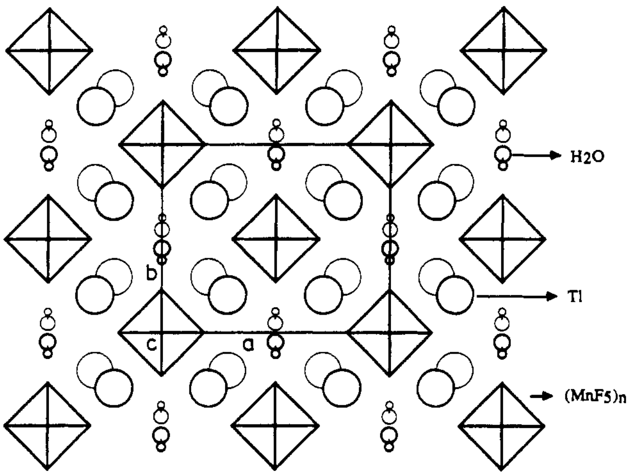

Figure 2. Projection of Tl_2MnF_5 structure of the *ab* plane. Water molecules and Tl atoms are shown in the interchain space.

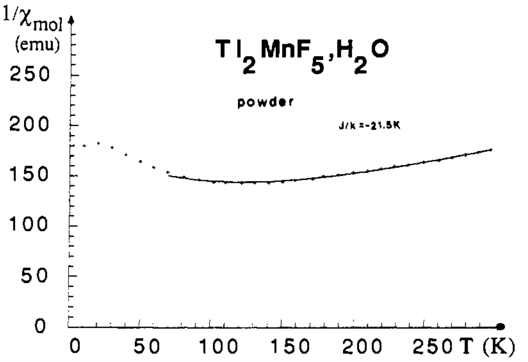

Figure 3. Temperature dependence of the reciprocal molar susceptibility for $Tl_2MnF_5{\cdot}H_2O$ from powder samples. The solid line corresponds to the best fitting with eq 2.

In the course of the magnetic and neutron diffraction investigation the question arose whether a crystallographic phase transition might have occurred at very low temperatures. Guinier patterns recorded at decreasing temperatures from 298 to 8 K did not show a line splitting and no superstructure reflections appeared. The lattice constants at 8 K were a = 9.537 (4) Å, b = 7.875 (2) Å, and c = 8.317 (2) Å. Thus there is no phase transition but, as expected for a linear chain structure, a strongly anisotropic thermal expansion is observed in the *ab* plane with the coefficients α of 4.74×10^{-5} along the *a*-axis and 5.56×10^{-5} along the *b*-axis but 0.91×10^{-5} along the *c*-axis (assuming linearity between 8 and 298 K).

Magnetic Properties of $Tl_2MnF_5{\cdot}H_2O$. The temperature dependence of the reciprocal susceptibility of powder samples of $Tl_2MnF_5{\cdot}H_2O$ is given in Figure 3. The observed broad minimum is doubtless due to 1D short-range antiferromagnetic interactions within the chains. Above 200 K the compound obeys a Curie–Weiss law with Curie constant and extrapolated paramagnetic Curie temperature: $C_m = 4.3 \pm 0.1$ and $\Theta_p = -470 \pm 10$ K, respectively. The choice of the temperature range has a certain influence on the accuracy of these values as the straight part of the curve is only reached near room temperature. The exchange constant within a chain (J/k) has been calculated by fitting the experimental results to an antiferromagnetic model of finite linear chains with a $S = 2$ spin and isotropic Heisenberg hamiltonian.

Fisher[20] has proposed a general equation for classical spins, which was further adapted by Smith and Friedberg[21] with the following formulation:

$$\chi_{(T)} = \frac{Ng^2\beta^2S(S+1)}{3kT}\,\frac{(1+u)}{(1-u)} \qquad (1)$$

$$u = \coth K - \frac{1}{K} \qquad K = \frac{2JS(S+1)}{kT}$$

Table IV. Structural and Magnetic Parameters of Pentafluoromanganates

compound	Mn–F–Mn angle, deg	Mn–Mn dist, Å	Θ_p, K	C_m	J/k, K	g	ref
$K_2MnF_5{\cdot}H_2O$	163.3	4.09	−295	3.95	−18.2	2.06	2
$Rb_2MnF_5{\cdot}H_2O$	176.0	4.17	−445	4.54	−21.8	2.09	2
			−428		−20.0	2.02	3
$Cs_2MnF_5{\cdot}H_2O$	180.0	4.25	−360	4.41	−17.9	2.04	2
			−331		−19.0	2.01	3
$Tl_2MnF_5{\cdot}H_2O$	179.2	4.17	−470	4.30	−21.5	1.99	*a*

[a] This work.

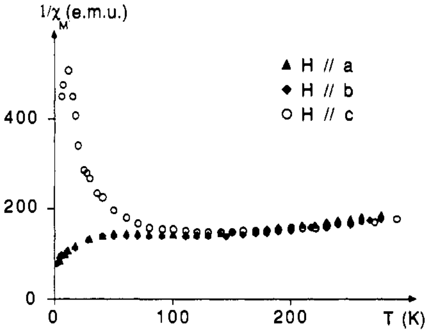

Figure 4. Temperature dependence of the reciprocal molar susceptibility for $Tl_2MnF_5{\cdot}H_2O$ with H successively parallel to the three crystallographic axes.

For antiferromagnetic Heisenberg chains of finite length a more general equation has been proposed[20]

$$\chi_{(T)} = \frac{Ng^2\beta^2S(S+1)}{(n+1)3kT}\left[(n+1)\frac{1+u}{1-u} - 2u\frac{1-u^{n+1}}{(1-u)^2}\right] \qquad (2)$$

where $(n + 1)$ is the number of spins per chain. If $n + 1$ is a large odd number and if $J < 0$, eq 2 leads to a result quite similar to that given by eq 1, except that, for decreasing temperatures, a susceptibility increase is observed for sufficiently low temperatures. Interchain long-range ordering is not taken into account in both equations.

As shown in Figure 3 for powder samples, a fitting between experimental data and the calculated curve is achieved for $T >$ 80 K by using in eq 2 the following constants: $J/k = -21.5$ K, $g = 1.99$, and $(n + 1) = 1000$.

The magnetic parameters provided from powder experiments are in good agreement with those obtained for the isostructural $Rb_2MnF_5{\cdot}H_2O$ and $Cs_2MnF_5{\cdot}H_2O$ phases, as shown in Table IV. The broad minimum which occurs around 100–150 K in the $\chi^{-1} = f(T)$ curve (Figure 3) is the signature of low-dimensional interactions.

The magnetic investigation on single crystals has clearly demonstrated the anisotropy of the magnetic interactions. The shape of the thermal variation of the magnetic susceptibility depends on the direction of the applied field relative to the axes of the orthorhombic unit cell as shown in Figure 4. When the magnetic field is applied parallel to the chain direction, i.e. to the *c*-axis, the increase of the reciprocal susceptibility for decreasing temperatures down to 10 K is similar to that which could be expected for χ. In the same way the plateau which is observed down to $T \approx 40$ K when H is parallel, either to the *a*- or the *b*-axis could be associated with $\chi_{\perp}$. These results are actually in good agreement with the magnetic structure, as shown hereafter. However, one may notice that it is not possible to conclude unambiguously the presence of 3D-ordering temperature only on the basis of magnetic data.

Magnetic Structure of $Tl_2MnF_5{\cdot}H_2O$. Neutron diffraction patterns of $Tl_2MnF_5{\cdot}H_2O$ at 30 and at 2 K are shown in Figure 5 together with their corresponding difference pattern. At 2 K one observes new peaks which can be attributed to a 3-D magnetic ordering. These peaks can be indexed in the same cell as the nonmagnetic one.

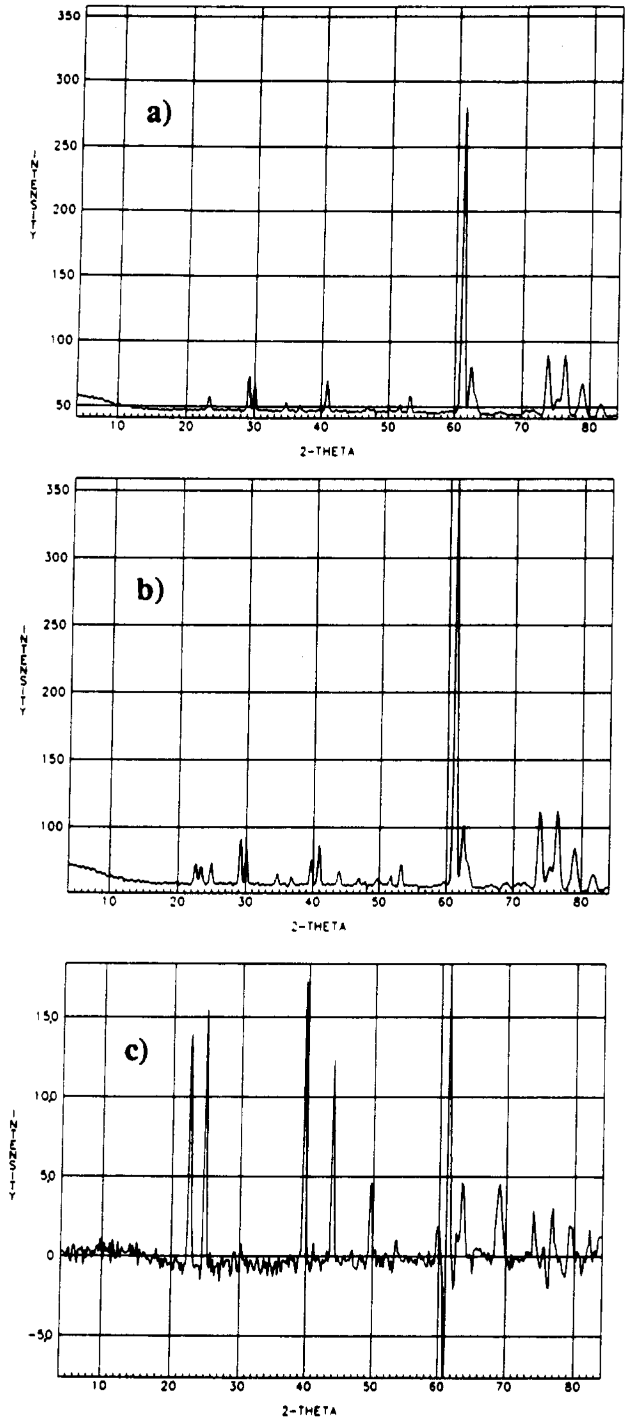

Figure 5. Neutron diffraction patterns of $Tl_2MnF_5 \cdot H_2O$ at (a) 30 K and (b) at 2 K and (c) the difference pattern.

Table V. Atomic Coordinates for $Tl_2MnF_5 \cdot H_2O$ at 30 K

space group: *Cmcm* $b = 7.861$ (1) Å
$a = 9.526$ (2) Å $c = 8.317$ (1) Å

atom	*x*	*y*	*z*	*B*,[a] Å^2
Tl	0.2093 (6)	0.2961 (8)	0.25	0.56 (4)
Mn	0	0	0	0.60 (4)
F1	0	−0.014 (2)	0.25	0.87 (5)
F2	0.191 (1)	0	0	0.87[b]
F3	0	0.239 (2)	0.015 (1)	0.87[b]
O	0.5	0.056 (2)	0.25	0.87[b]
H	0.5	0.126 (3)	0.152 (2)	0.87[b]

[a] *B* values are isotropic thermal factors. [b] The same temperature factor has been attributed to the F, O, and H atoms.

Table VI. Observed and Calculated Magnetic Intensities of $Tl_2MnF_5 \cdot H_2O$ at 2 K

hkl	I_{obs}	I_{calc}	*hkl*	I_{obs}	I_{calc}
101	7362	6886	321	2576	2352
011	6766	6848	231	1456	1904
211	7956	7240	123	524	744
121	5536	5856	411	1384	1864
301	2340	2212	303	344	364
031	1788	1384			

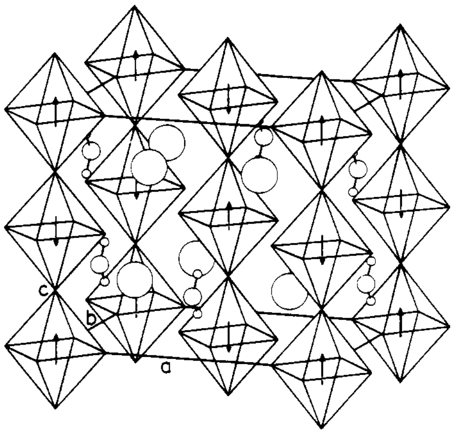

Figure 6. Proposed magnetic structure of $Tl_2MnF_5 \cdot H_2O$ showing the antiferromagnetic spin arrangement within a chain.

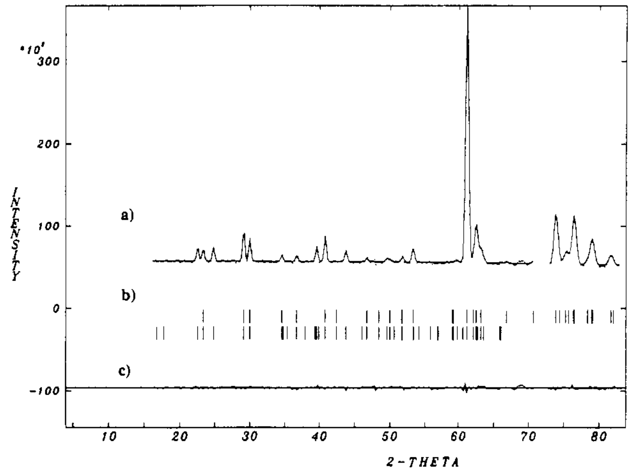

Figure 7. Refined neutron diffraction pattern of $Tl_2MnF_5 \cdot H_2O$ at T = 2 K: (a) calculated profile intensities (full line); (b) positions of nuclear peaks (above) and magnetic peaks (below); (c) difference spectrum.

At 30 K the structure has been refined in the *Cmcm* space group using only isotropic temperature factors down to a *R* value of 0.034. The corresponding structural parameters are reported in Table V. There are no important differences with the results obtained at 300 K in the XRD determination except for the position of the hydrogen atoms.

At 2 K the manganese atoms composing the unit cell have been called Mn_1 to Mn_4 with the corresponding crystallographic positions: Mn_1, (0, 0, 0); Mn_2, (0, 0, $^1/_2$); Mn_3, ($^1/_2$, $^1/_2$, 0); Mn_4, ($^1/_2$, $^1/_2$, $^1/_2$). Each manganese atom has S_i spin ($i = 1$–4).

The loss of the *C* lattice translation seen from the indices of the magnetic reflections leads to an antiferromagnetic arrangement between both the Mn_1 and Mn_3 moments as well as the Mn_2 and Mn_4 moments. We have calculated all the possible colinear magnetic arrangements in the *Pm'cm* space group. The best fitting has been obtained with the moments parallel to the *c*-axis and with the following sequence: $+S_1 - S_2 - S_3 + S_4$. The moment per manganese atom as calculated from this model is 3.2 ± 0.2 μ_B. The intensities have been reported in Table VI and the magnetic structure in Figure 6. The relative high value of the reliability factor $R = 9.2\%$ and the low value of the magnetic moment can result from a nonclassic manganese magnetic form factor as already encountered in low-dimensional systems and from a lack of cohesion in the magnetic chains. The refined neutron

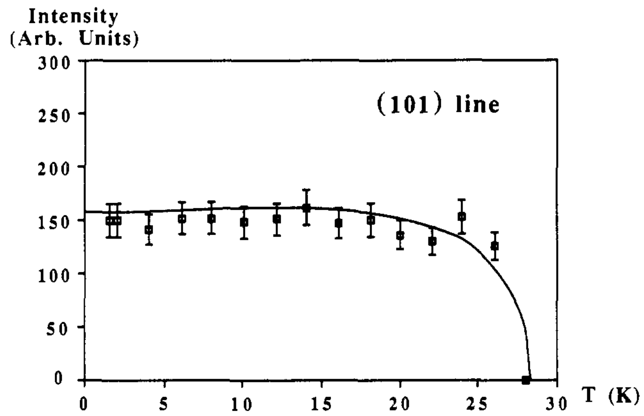

Figure 8. Temperature dependence of (101) line intensity.

diffraction pattern corresponding to that hypothesis is given in Figure 7. The variation of the intensity of the (101) magnetic line vs. temperature is given in Figure 8 and leads to an ordering temperature of $T_N = 28 \pm 1$ K.

Conclusions

We may conclude from this investigation that the linear chain hydrated fluoride $Tl_2MnF_5{\cdot}H_2O$ behaves as a 1D magnetic material like the other already investigated $A_2MF_5{\cdot}H_2O$ compounds. Within the infinite $(MnF_5)_n^{2n-}$ chains, MnF_6 octahedra are characterized by elongated Mn–F bridging distances enhanced by a Jahn–Teller effect associated with high-spin Mn(III). In the Tl phase the bridging angle β is close to the optimum 180° value, β(Mn–F–Mn) = 179.2°, and the corresponding intrachain exchange constant J/k (approximately −22 K) is in good agreement with the previously proposed dependence of J/k on $\cos^2 \beta$. Therefore, within a large temperature range ($70 \lesssim T \lesssim 300$ K), the prevailing coupling mechanism is an antiparallel intrachain coupling via σ superexchange, whereas below T_N = 28 K the magnetic chains participate in 3D interactions.

Acknowledgment. We are indebted to J. Grannec for fruitful comments. This work has been carried out in the scope of an EEC Research Program. One of us (P.N.) thanks the Government of the Canary Islands for a grant. We also wish to thank W. Abriel for having performed the low-temperature powder diffractogram measurements and for helpful discussions.

Registry No. $Tl_2MnF_5{\cdot}H_2O$, 138604-22-5.

Supplementary Material Available: Tables of experimental data for the crystal structure determination and anisotropic thermal parameters (2 pages); a listing of observed and calculated structure factors (3 pages). Ordering information is given on any current masthead page.

Contribution from the Department of Inorganic Chemistry, Faculty of Sciences, University of Granada, Granada, Spain,
Laboratoire de Chimie de Coordination du CNRS, UP 8241 liée par conventions à l'Université Paul Sabatier
et à l'Institut National Polytechnique, 205 route de Narbonne, 31077 Toulouse Cedex, France,
and Division of Inorganic Chemistry, Department of Chemistry, University of Helsinki, Vuorikatu 20, SF-00100 Helsinki, Finland

Structural and Magnetic Studies of a Syn-Anti Carboxylate-Bridged Helix-like Chain Copper(II) Complex

Enrique Colacio,*[†] José-Manuel Dominguez-Vera,[‡] Jean-Pierre Costes,[‡] Raikko Kivekäs,[§]
Jean-Pierre Laurent,*[‡] José Ruiz,[†] and Markku Sundberg[§]

Received May 6, 1991

The preparation, magnetic properties, and crystal and molecular structure of $[CuL(H_2O)]_n$ are described (L stands for the doubly deprotonated form of 1,3-dimethyl-5-((2-carboxyphenyl)azo)barbituric acid). The crystals are orthorhombic, of space group $P2_12_12_1$, with cell constants $a = 8.171$ (1) Å, $b = 10.302$ (3) Å, $c = 17.006$ (5) Å, and $Z = 4$. The structure was solved and refined to $R = 0.052$. The copper(II) ions are in a distorted square-pyramidal environment. They are sequentially bridged by carboxylate groups in the syn-anti conformation, resulting in the formation of infinite zigzag (or helix-like?) chains running parallel to the a axis. From magnetic susceptibility measurements, the complex is found to exhibit ferromagnetic intrachain interactions with an exchange coupling of $J/k = 4.8$. Magnetic and structural parameters of this and other related complexes are compared, and some magneto–structural trends are discussed.

Introduction

Historically, antiferromagnetic exchange coupling in a dinuclear complex was first observed in $Cu_2(CH_3COO)_4{\cdot}2H_2O$, in which two copper(II) ions are bridged symmetrically by four acetate groups.[1,2] Subsequently a variety of related complexes[3-5] were considered, all displaying substantial antiferromagnetic interactions. This behavior has been theoretically rationalized at various levels of sophistication,[6,7] but it is obvious empirically that these strong antiferromagnetic interactions have to be related to the syn-syn configuration adopted by the triatomic O–C–O bridges.

Indeed, much smaller (antiferro- or ferromagnetic) interactions were found for complexes in which syn-anti bridges are operative.[8-13] It may be noted that structurally characterized examples of this syn-anti configuration are to date far less numerous than those with the syn-syn configuration. This is unfortunate since, due to their geometry, syn-anti bridges would allow a great variety of structural and magnetic characteristics to be observed.

A good strategy to force RCO_2^- groups to adopt the syn-anti configuration would be their incorporation into a polydentate

---

[†] University of Granada.

[‡] Laboratoire de Chimie de Coordination du CNRS.

[§] University of Helsinki.

(1) Bleaney, B.; Bowers, K. D. *Proc. R. Soc. London, A* **1952**, *214*, 451.
(2) Figgis, B. N.; Martin, R. L. *J. Chem. Soc.* **1956**, 3837.
(3) Doedens, R. J. *Prog. Inorg. Chem.* **1976**, *21*, 209.
(4) Melnik, M. *Coord. Chem. Rev.* **1982**, *42*, 259.
(5) Kato, M.; Muto, Y. *Coord. Chem. Rev.* **1988**, *92*, 45.
(6) Albonico, C.; Bencini, A. *Inorg. Chem.* **1988**, *27*, 1934 and references therein.
(7) de Loth, P.; Cassoux, P.; Daudey, J.-P.; Malrieu, J.-P. *J. Am. Chem. Soc.* **1981**, *103*, 4007.
(8) Corvan, P. J.; Estes, W. E.; Weller, R. R.; Hatfield, W. E. *Inorg. Chem.* **1980**, *19*, 1297.
(9) Carling, R. L.; Kopinga, K.; Kahn, O.; Verdaguer, M. *Inorg. Chem.* **1986**, *25*, 1786.
(10) Towle, D. K.; Hoffmann, S. K.; Hatfield, W. E.; Singh, P.; Chaudhuri, P. *Inorg. Chem.* **1988**, *27*, 394.
(11) Levstein, P. R.; Calvo, R. *Inorg. Chem.* **1990**, *29*, 1581.
(12) Colacio, E.; Costes, J.-P.; Kivekas, R.; Laurent, J.-P.; Ruiz, J. *Inorg. Chem.* **1990**, *29*, 4240 and references therein.
(13) Coughlin, P. K.; Lippard, S. J. *J. Am. Chem. Soc.* **1984**, *106*, 2328.

0020-1669/92/1331-0774$03.00/0